

Decoding Event-related Potential from Ear-EEG Signals based on Ensemble Convolutional Neural Networks in Ambulatory Environment

Young-Eun Lee
Dept. Brain and Cognitive Engineering
Korea University
Seoul, Republic of Korea
ye_lee@korea.ac.kr

Seong-Whan Lee
Dept. Artificial Intelligence
Korea University
Seoul, Republic of Korea
sw.lee@korea.ac.kr

Abstract—Recently, practical brain-computer interface is actively carried out, especially, in an ambulatory environment. However, the electroencephalography (EEG) signals are distorted by movement artifacts and electromyography signals when users are moving, which make hard to recognize human intention. In addition, as hardware issues are also challenging, ear-EEG has been developed for practical brain-computer interface and has been widely used. In this paper, we proposed ensemble-based convolutional neural networks in ambulatory environment and analyzed the visual event-related potential responses in scalp- and ear-EEG in terms of statistical analysis and brain-computer interface performance. The brain-computer interface performance deteriorated as 3–14% when walking fast at 1.6 m/s. The proposed methods showed 0.728 in average of the area under the curve. The proposed method shows robust to the ambulatory environment and imbalanced data as well.

Index Terms—brain-computer interface, ambulatory environment, ear-EEG, event-related potential, ensemble CNN

I. INTRODUCTION

Brain-computer interfaces (BCIs) in ambulatory environment are one of the most important consideration in real life. Although many researchers have studied BCI to recognize human cognitive state or intention based on brain signals such as electroencephalography (EEG), there are limitations in processing brain signals in ambulatory environments [1], [2]. Artifacts in the ambulatory environment distort the brain signals, lowering the accuracy and signal-to-noise ratio (SNR) of critical components, including human intention [3]–[5]. Therefore, they have attempted to decode human intention in the ambulatory environment using movement artifact removal methods [5]–[8] and deep neural networks [8]–[12].

Development of EEG measuring devices that can be used in real life to measure EEG signals have been actively conducted [13], [14]. Among them, ear-EEG has recently been

This work was partly supported by Institute for Information & Communications Technology Planning & Evaluation (IITP) grant funded by the Korea government (MSIT) (No. 2017-0-00451, Development of BCI based Brain and Cognitive Computing Technology for Recognizing User's Intentions using Deep Learning), (No. 2015-0-00185, Development of Intelligent Pattern Recognition Softwares for Ambulatory Brain Computer Interface), and (No. 2019-0-00079, Artificial Intelligence Graduate School Program (Korea University)).

extensively investigated by many researchers to increase user convenience, and has been verified by analyzing signal quality and implementing various BCI paradigms [13]. In addition, conventional scalp-EEG annoys users due to the high cost and difficulty of setting, such as using conductive gel for hair that needs to be washed after measurement and wearing a prominent cap [14]. In order to reduce the annoyance, simple and convenient devices were designed, such as Emotive EPOC and ear-EEG. Kidmose et al. [15] analyzed the scalp and ear-EEG signals using steady-state and transient event-related potential (ERP) paradigms. In addition, Debener et al. [13], [16] designed cEEGrid to placed electrodes around the ear, which can preserve the ERP components and have a similar performance to scalp-EEG. On the other hand, due to the limitation of lower performance than conventional scalp-EEG, several studies have attempted to increase the performance of ear-EEG for visual or auditory responses [14].

The BCI paradigms was developed primarily with motor imagery [17]–[20], ERP [21]–[25], and steady-state visual evoked potential (SSVEP) [4], [9], [25]–[27]. ERP and SSVEP are widely used in recognizing human intentions because they have a relatively large pattern of EEG signals as a visual response and show reliable performance in terms of accuracy and response time with a small number of EEG channels compared to other BCI paradigms [4], [24]. ERP is a time-locked brain response to certain types of stimuli (i.e. visual, auditory, haptic, etc.), with a particularly strong positive peak response, called P300, 300 msec after the appearance of a stimulus. In particular, it is mainly used because it rarely causes eye fatigue, low BCI illiteracy, and relatively high accuracy compared to other stimuli-based paradigms [26]. ERP evaluation proceeds with area under the curve (AUC) rather than accuracy because the ratio of each class is different, and SNR for signal quality evaluation proceeds.

There have been several attempts to use machine learning methods to recognize human intentions from visual responses. Castermans et al. [3] classified ERP intentions in the ambulatory environment up to 1.25 m/s using linear discriminant analysis classifier. Moreover, deep neural networks consisting

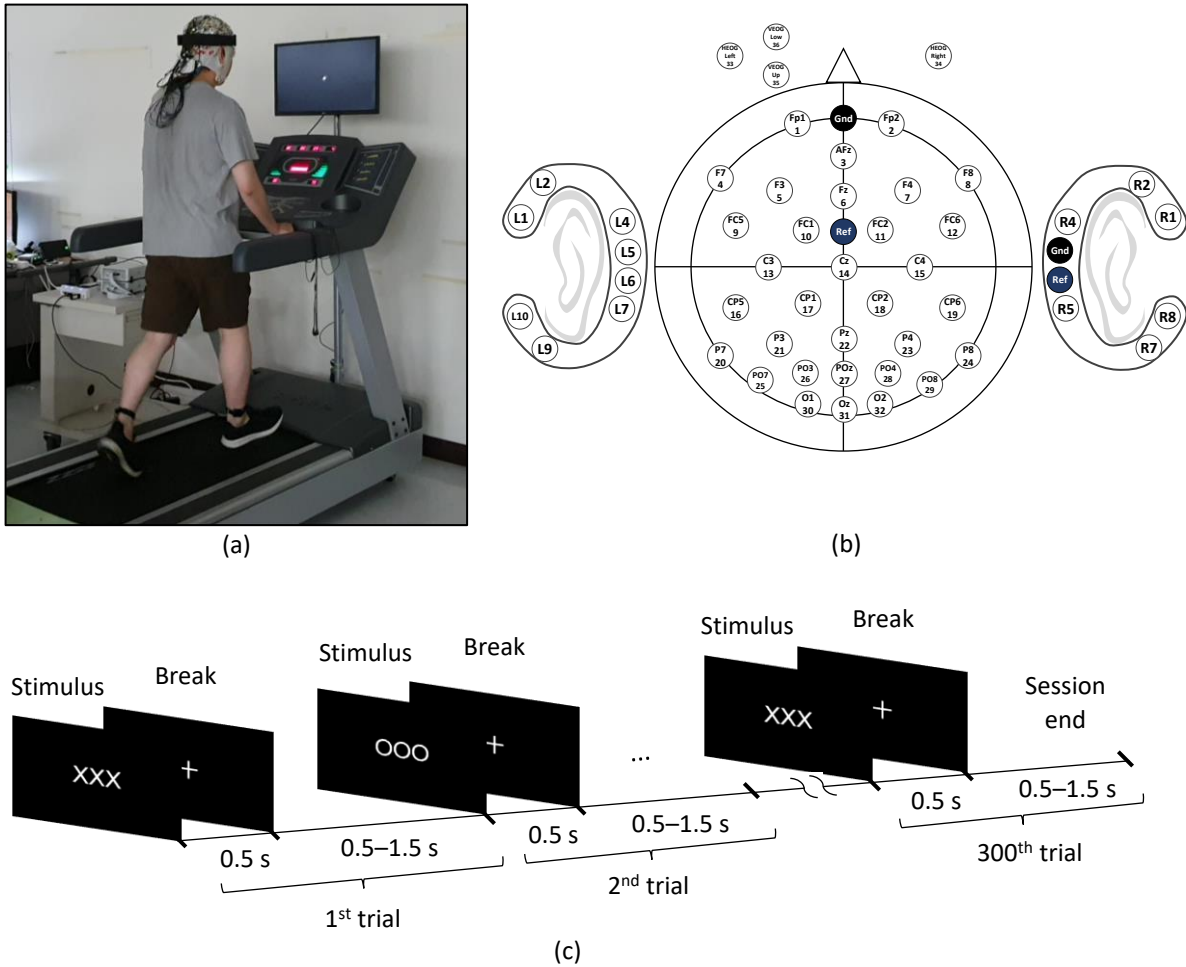


Fig. 1. Design of the experiment. (a) Experimental setup and recorders. Subjects walked on a treadmill and watched a display presenting stimuli of BCI paradigms. Signals from scalp-EEG, ear-EEG around both ears, EOGs placed above and below the left eye to measure the vertical EOGs (VEOGs) and on left and right temples to measure the horizontal EOGs (HEOGs), and IMU sensors comprising nine channels, including three-axis accelerometers, three-axis gyroscopes, and three-axis magnetometers, placed on the forehead, and left and right ankles were recorded during the experiments. (c) ERP paradigm consisting of 300 trials in a session, which presents target ‘OOO’ or non-target ‘XXX’ for 0.5 s, and takes a random rest for 0.5–1.5 s. Target and non-target appear in random order, with the target ratio of 0.2.

of convolutional neural networks (CNNs) has been proposed to detect the ERP responses [28]. However, ERP responses typically consist of different number of trials, with different ratios of target and non-target stimuli. Thus, training with a normal deep neural network results in lower AUC by increasing the number of predictions towards non-targets.

In this paper, we decoded the ERP responses from cap-EEG and ear-EEG in the ambulatory environment. For practical BCIs, simple hardware and high accurate classifier of human intention is necessary. To solve the imbalanced problem of target and non-target ratio in ERP paradigm, we used ensemble architecture by combining results from the separated data of non-target [29]–[31]. Therefore, we investigated ensemble-based convolutional neural networks to increase human intention recognition and used ear-EEG for practical BCI in the real-world.

II. MATERIALS AND METHODS

A. Participants

We included fifteen healthy participants (2 females, age 24.8 ± 3.4 years) with normal or corrected-to-normal vision and no difficulties to walk at Korea University in Seoul, Korea. None of the participants had a history of neurological, psychiatric, or any other pertinent disease that otherwise might have affected the experimental results. This study was reviewed and approved by the Korea University Institutional Review Board (KUIRB-2019-0194-01).

B. Experimental Paradigm

The subjects were stood on the treadmill at $80 (\pm 5)$ cm in front of a 60 Hz LCD monitor (Samsung, SyncMaster 2494HM, refresh rate: 60 Hz; resolution: 1920×1080) and walked at two different speeds (0.8 and 1.6 m/s). We experimented with target (‘OOO’) and non-target (‘XXX’) stimuli ERP paradigm with the target ratio of 0.2. The number

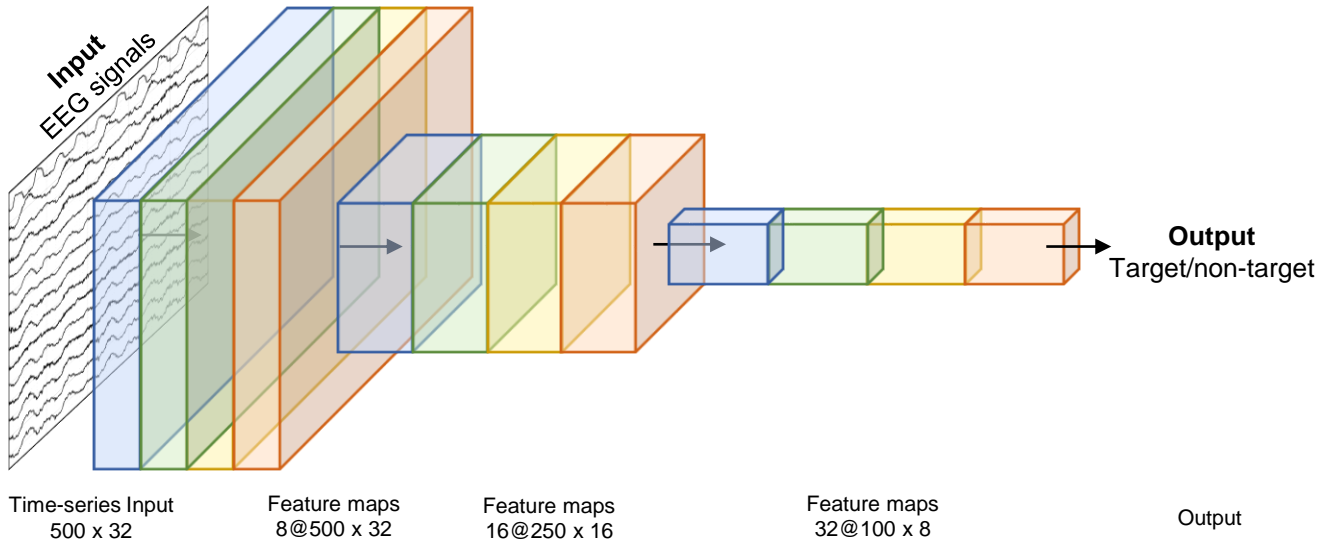


Fig. 2. Proposed method architecture. The EEG signals are the input of the architecture, and the output is the classes, target or non-target. Each colored block indicates each ensemble network module.

of total trials was 300, including 60 target trials. The stimuli presented for 0.5 s and the rest time was randomly 0.5–1.5 s. The visual stimuli were generated using the Psychophysics Toolbox in Matlab. We followed the ERP paradigm of a previous study [32].

C. Data Acquisition and Preprocessing

Fig. 1 shows the experimental setup about measurement, experimental tools, and channel placement. We recorded 32-channel of cap-EEG, 18-channels of ear-EEG, and 9-channels Inertial Measurement Unit (IMU) sensors. We used a wireless interface (MOVE system, Brain Product GmbH) and Ag/AgCl electrodes to acquire EEG signals from the scalp and Smarting System (mBrainTrain LLC) and cEEGrid electrodes to acquire EEG signals from ear. Three wearable IMU sensors have recorded the movement on the head, left and right ankles. The cap electrodes were placed according to the 10-20 international system at locations: Fp1, Fp2, AFz, F7, F3, Fz, F4, F8, FC5, FC1, FC2, FC6, C3, Cz, C4, CP5, CP1, CP2, CP6, P7, P3, Pz, P4, P8, PO7, PO3, POz, PO4, PO8, O1, Oz, and O2. Ear-EEG electrodes were cEEGrid, having 10 channels on left side (L1 to L10), 8 channels on right side (R1 to R8) and GND and REF in the middle of right side. The impedances were maintained below 10 $k\Omega$ for both scalp and ear-EEG. We set the sampling rate as 500 Hz for cap and ear-EEG and 128 Hz for IMU sensors. The dataset is published in 2020 International BCI Competition dataset storage (<https://osf.io/pq7vb/>).

All BCI experiments were developed based on the OpenBMI [33], BBCI [34] and Psychophysics toolboxes [35]. We performed down sampling or resampling to 100 Hz for all measurement and high-pass filter using finite impulse response filter passing above 3 Hz.

D. Proposed Method

We used ensemble-based CNNs to train ERP responses described in Fig. 2. Ensemble networks are to combine the predictions of several base predictors (each colored block in Fig. 2) constructed with a given learning algorithm in order to improve generality or robustness over a single predictors. Since the ratio of target and non-target is 0.2, the non-target data was divided into four groups. Each ensemble model forwarded with one group of non-target data and target data, and then the models averaged the gradients of all four groups to update the weights of model.

The neural networks are three CNN-hidden layers and a fully-connected hidden layers. In the first layer, eight kernels, channel-wise convolution, having a size of 1 by the number of channels are used and the feature maps have a shape of time by 1. The feature maps are calculated by

$$x_k = f(\sigma_k(p)) \quad (1)$$

where σ_k is convolutional function, p is a position of input, $f(\cdot)$ function is activation function, rectified linear unit (ReLU) is used for the activation function and is denoted by

$$f(z) = \max(0, z) \quad (2)$$

The convolutional function σ_k can be represented by

$$\sigma_k(p) = b_k + \sum_{i=1}^{K_x} \sum_{j=1}^{K_y} x^{i,j} \times w_k^{i,j} \quad (3)$$

where b_k is bias of kernel k , K_x and K_y is kernel size, x is input matrix, and w_k is weight of kernel k .

Cross-entropy loss, logarithm multiplying classes, are used for the loss function of the algorithm, which is denoted by

$$\text{loss} = -t \times \log(F(s)) - (1 - t) \times \log(1 - F(s)) \quad (4)$$

TABLE I
THE AUC OF SCALP-EEG AND EAR-EEG FOR ALL SUBJECTS

| Scalp-EEG | Subject | S1 | S2 | S3 | S4 | S5 | S6 | S7 | S8 | S9 |
|-----------|---------|-------|-------|-------|-------|-------|-------|-------------|-------|-------|
| | AUC | 0.900 | 0.802 | 0.776 | 0.890 | 0.674 | 0.817 | 0.709 | 0.486 | 0.759 |
| Ear-EEG | Subject | S10 | S11 | S12 | S13 | S14 | S15 | Average | | |
| | AUC | 0.597 | 0.730 | 0.716 | 0.652 | 0.618 | 0.796 | 0.728±0.108 | | |
| Scalp-EEG | Subject | S1 | S2 | S3 | S4 | S5 | S6 | S7 | S8 | S9 |
| | AUC | 0.592 | 0.669 | 0.573 | 0.663 | 0.738 | 0.574 | 0.514 | 0.545 | 0.731 |
| Ear-EEG | Subject | S10 | S11 | S12 | S13 | S14 | S15 | Average | | |
| | AUC | 0.565 | 0.618 | 0.704 | 0.679 | 0.338 | 0.477 | 0.599±0.103 | | |

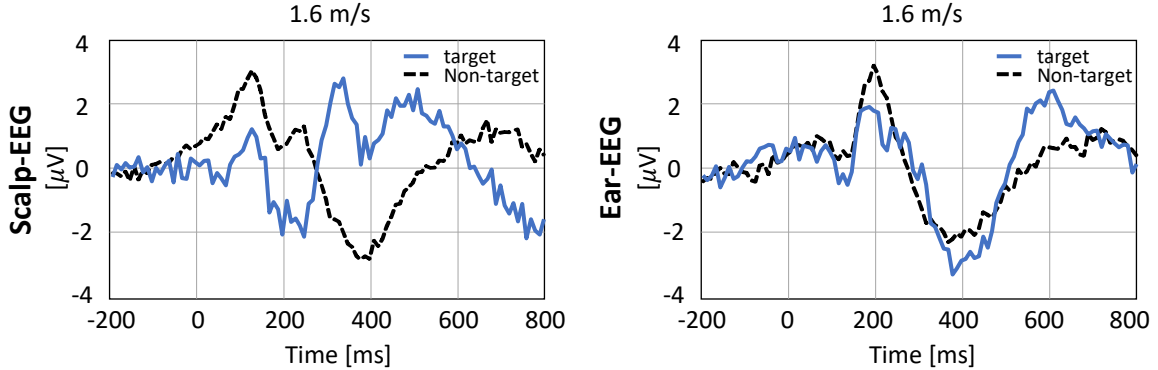


Fig. 3. ERP waves of scalp- and ear-EEG at 1.6 m/s. The plots show the grand average of the target and non-target responses indicated in blue and black line, respectively.

where t is a class in $[0, 1]$, s is the ground truth, and $F(\cdot)$ is prediction function. The learning rate was 0.01 and weights were initialized with a normal distribution. The number of epochs was 50 and batch size was 32.

III. RESULTS AND DISCUSSION

For evaluating our proposed methods, we used AUC as the metric due to different number of target and non-target. The results were statistically analyzed using the statistical method of t-test. Table I shows the results of analysis for ERP from scalp and ear-EEG and indicates all subjects' performance for each method. Fig. 3 shows the results of the ERP responses from scalp- and ear-EEG, plotting the target and non-target waves.

A. Ensemble Module

We used an ensemble module which can improve the performance when training imbalanced data. The ensemble module trained partitioned data set consisting of four non-target data set and the full target data set. The separated ensemble model forwarded the data, and then calculated the gradients of weights by averaging the gradients from all ensemble models. The total model weights were updated with all non-target and target data set at once. The AUC of proposed method was 0.728 ± 0.108 in average for all subject.

B. ERP Responses

Fig. 3 shows the ERP responses of scalp and ear-EEG with the target and non-target responses. In scalp-EEG, the differ-

ence between target and non-target was huge, in particularly around at 300 ms. Whereas the ERP responses from ear-EEG were apparent, the difference between target and non-target in ear-EEG was comparatively inferior. The ERP responses in ear-EEG showed the possibility to use practical BCI in the ambulatory environment.

IV. CONCLUSION

In this study, we proposed an ensemble CNN architecture in ambulatory environment decoding visual ERP responses in scalp- and ear-EEG. As practical BCIs require a robust system in an ambulatory environment and simple hardware usable in the real-world, we show that the proposed method improved the BCI performance in the ambulatory environment. The results for recognizing human intention in an ambulatory environment without using artifact removal methods had the reasonable performance although the data set was imbalanced. However, the performances were lower that could not fit network because of the artifacts' variance. In conclusion, we showed that ensemble-based convolutional neural networks could show reasonable performance even in the ambulatory environment. However, it was difficult to increase the performance fitting from training data in standing condition to test data in walking condition due to huge artifacts features. In the future, the study removing noisy signals but remaining essential components was necessary to recognize the human intention for a different session in the ambulatory environment.

ACKNOWLEDGMENT

The authors would like to thank N.-S. Kwak for his help with the design of experimental setting, M. Lee and J.-H. Jeong for their help with advising the research, and G.-H. Shin for his assistance with data collection.

REFERENCES

- [1] T. P. Luu, S. Nakagome, Y. He, and J. L. Contreras-Vidal, "Real-time EEG-based brain-computer interface to a virtual avatar enhances cortical involvement in human treadmill walking," *Sci. Rep.*, vol. 7, no. 1, p. 8895, Aug. 2017.
- [2] T. P. Luu, Y. He, S. Nakagome, J. Gorges, K. Nathan, and J. L. Contreras-Vidal, "Unscented kalman filter for neural decoding of human treadmill walking from non-invasive electroencephalography," in *Proc. 38th Annu. Int. Conf. IEEE Engineering in Medicine and Biology Society (EMBC)*, Orlando, USA, Aug. 2016, pp. 1548–1551.
- [3] T. Castermans, M. Duvinage, M. Petieau, T. Hoellinger, C. De Saedeleer, K. Seetharaman, A. Bengoetxea, G. Cheron, and T. Dutoit, "Optimizing the performances of a P300-based brain-computer interface in ambulatory conditions," *IEEE J. Emerg. Sel. Topics Circuits Syst.*, vol. 1, no. 4, pp. 566–577, Dec. 2011.
- [4] N.-S. Kwak, K.-R. Müller, and S.-W. Lee, "A lower limb exoskeleton control system based on steady state visual evoked potentials," *J. Neural Eng.*, vol. 12, no. 5, p. 056009, Aug. 2015.
- [5] Y.-E. Lee, N.-S. Kwak, and S.-W. Lee, "A real-time movement artifact removal method for ambulatory brain-computer interfaces," *IEEE Trans. Neural Syst. Rehabil. Eng.*, Nov. 2020.
- [6] K. Gramann, J. T. Gwin, N. Bigdely-Shamlo, D. P. Ferris, and S. Makeig, "Visual evoked responses during standing and walking," *Front. Hum. Neurosci.*, vol. 4, p. 202, Oct. 2010.
- [7] T. C. Bulea, J. Kim, D. L. Damiano, C. J. Stanley, and H.-S. Park, "Pre-frontal, posterior parietal and sensorimotor network activity underlying speed control during walking," *Front. Hum. Neurosci.*, vol. 9, p. 247, May 2015.
- [8] A. D. Nordin, W. D. Hairston, and D. P. Ferris, "Dual-electrode motion artifact cancellation for mobile electroencephalography," *J. Neural Eng.*, vol. 15, no. 5, p. 056024, Aug. 2018.
- [9] N.-S. Kwak, K.-R. Müller, and S.-W. Lee, "A convolutional neural network for steady state visual evoked potential classification under ambulatory environment," *PloS One*, vol. 12, no. 2, p. e0172578, Feb. 2017.
- [10] M. Lee, R. D. Sanders, S.-K. Yeom, D.-O. Won, K.-S. Seo, H. J. Kim, G. Tononi, and S.-W. Lee, "Network properties in transitions of consciousness during propofol-induced sedation," *Sci. Rep.*, vol. 7, no. 1, pp. 1–13, Dec. 2017.
- [11] O.-Y. Kwon, M.-H. Lee, C. Guan, and S.-W. Lee, "Subject-independent brain-computer interfaces based on deep convolutional neural networks," *IEEE Trans. Neural Netw. Learn. Syst.*, vol. 31, no. 10, pp. 3839–3852, Nov. 2019.
- [12] Y.-E. Lee and M. Lee, "Decoding visual responses based on deep neural networks with ear-EEG signals," in *Proc. 8th Int. Winter Conf. IEEE Brain-Comput. Interf.*, Jeongseon, Republic of Korea, Feb. 2020, pp. 1–6.
- [13] M. G. Bleichner and S. Debener, "Concealed, unobtrusive ear-centered EEG acquisition: cEEGrids for transparent EEG," *Front. Hum. Neurosci.*, vol. 11, p. 163, Apr. 2017.
- [14] N.-S. Kwak and S.-W. Lee, "Error correction regression framework for enhancing the decoding accuracies of ear-EEG brain-computer interfaces," *IEEE Trans. Cybern.*, pp. 1–14, Jul. 2019.
- [15] P. Kidmose, D. Looney, M. Ungstrup, M. L. Rank, and D. P. Mandic, "A study of evoked potentials from ear-EEG," *IEEE Trans. Biomed. Eng.*, vol. 60, no. 10, pp. 2824–2830, May 2013.
- [16] S. Debener, R. Emkes, M. De Vos, and M. Bleichner, "Unobtrusive ambulatory EEG using a smartphone and flexible printed electrodes around the ear," *Sci. Rep.*, vol. 5, p. 16743, Nov. 2015.
- [17] H.-I. Suk and S.-W. Lee, "Subject and class specific frequency bands selection for multiclass motor imagery classification," *Int. J. Imaging Syst. Technol.*, vol. 21, no. 2, pp. 123–130, May 2011.
- [18] R. T. Schirmer, J. T. Springenberg, L. D. J. Fiederer, M. Glasstetter, K. Eggenberger, M. Tangermann, F. Hutter, W. Burgard, and T. Ball, "Deep learning with convolutional neural networks for eeg decoding and visualization," *Hum. Brain Mapp.*, vol. 38, no. 11, pp. 5391–5420, Aug. 2017.
- [19] J.-H. Kim, F. Bießmann, and S.-W. Lee, "Decoding three-dimensional trajectory of executed and imagined arm movements from electroencephalogram signals," *IEEE Trans. Neural Syst. Rehabil. Eng.*, vol. 23, no. 5, pp. 867–876, Dec. 2014.
- [20] M.-H. Lee, S. Fazli, J. Mehnert, and S.-W. Lee, "Subject-dependent classification for robust idle state detection using multi-modal neuroimaging and data-fusion techniques in BCI," *Pattern Recognit.*, vol. 48, no. 8, pp. 2725–2737, Aug. 2015.
- [21] S.-K. Yeom, S. Fazli, K.-R. Müller, and S.-W. Lee, "An efficient ERP-based brain-computer interface using random set presentation and face familiarity," *PloS One*, vol. 9, no. 11, p. e111157, Nov. 2014.
- [22] Y. Chen, A. D. Atnafu, I. Schlattner, W. T. Weldtsadik, M.-C. Roh, H. J. Kim, S.-W. Lee, B. Blankertz, and S. Fazli, "A high-security EEG-based login system with RSVP stimuli and dry electrodes," *IEEE Trans. Inf. Forensic Secur.*, vol. 11, no. 12, pp. 2635–2647, Jun. 2016.
- [23] D.-O. Won, H.-J. Hwang, D.-M. Kim, K.-R. Müller, and S.-W. Lee, "Motion-based rapid serial visual presentation for gaze-independent brain-computer interfaces," *IEEE Trans. Neural Syst. Rehabil. Eng.*, vol. 26, no. 2, pp. 334–343, Aug. 2017.
- [24] M.-H. Lee, J. Williamson, D.-O. Won, S. Fazli, and S.-W. Lee, "A high performance spelling system based on EEG-EOG signals with visual feedback," *IEEE Trans. Neural Syst. Rehabil. Eng.*, vol. 26, no. 7, pp. 1443–1459, May 2018.
- [25] M.-H. Lee, J. Williamson, Y.-E. Lee, and S.-W. Lee, "Mental fatigue in central-field and peripheral-field steady-state visually evoked potential and its effects on event-related potential responses," *Neuroreport*, vol. 29, pp. 1301–1308, Oct. 2018.
- [26] G. R. Muller-Putz, R. Scherer, C. Neuper, and G. Pfurtscheller, "Steady-state somatosensory evoked potentials: suitable brain signals for brain-computer interfaces?" *IEEE Trans. Neural Syst. Rehabil. Eng.*, vol. 14, no. 1, pp. 30–37, Mar. 2006.
- [27] D.-O. Won, H.-J. Hwang, S. Dähne, K.-R. Müller, and S.-W. Lee, "Effect of higher frequency on the classification of steady-state visual evoked potentials," *J. Neural Eng.*, vol. 13, no. 1, p. 016014, Dec. 2015.
- [28] V. J. Lawhern, A. J. Solon, N. R. Waytowich, S. M. Gordon, C. P. Hung, and B. J. Lance, "EEGNet: a compact convolutional neural network for EEG-based brain-computer interfaces," *J. Neural Eng.*, vol. 15, no. 5, p. 056013, Jul. 2018.
- [29] X. Tao, Q. Li, W. Guo, C. Ren, C. Li, R. Liu, and J. Zou, "Self-adaptive cost weights-based support vector machine cost-sensitive ensemble for imbalanced data classification," *Inf. Sci.*, vol. 487, pp. 31–56, Jun. 2019.
- [30] K. Yang, Z. Yu, X. Wen, W. Cao, C. P. Chen, H.-S. Wong, and J. You, "Hybrid classifier ensemble for imbalanced data," *IEEE Trans. Neural Netw. Learn. Syst.*, vol. 31, no. 4, pp. 1387–1400, Apr. 2019.
- [31] G. Wang, T. Zhou, K.-S. Choi, and J. Lu, "A deep-ensemble-level-based interpretable takagi-sugeno-kang fuzzy classifier for imbalanced data," *IEEE Trans. Cybern.*, Sep. 2020.
- [32] M.-H. Lee, O.-Y. Kwon, Y.-J. Kim, H.-K. Kim, Y.-E. Lee, J. Williamson, S. Fazli, and S.-W. Lee, "EEG dataset and OpenBMI toolbox for three BCI paradigms: An investigation into BCI illiteracy," *GigaScience*, vol. 8, no. 5, p. giz002, Jan. 2019.
- [33] M.-H. Lee, K.-T. Kim, Y.-J. Kee, J.-H. Jeong, S.-M. Kim, S. Fazli, and S.-W. Lee, "OpenBMI: A real-time data analysis toolbox for brain-machine interfaces," in *Proc. IEEE Int. Conf. Syst. Man Cybern. (SMC)*, Jeongseon, Republic of Korea, Oct. 2016, pp. 884–887.
- [34] R. Krepek, B. Blankertz, G. Curio, and K.-R. Müller, "The Berlin Brain-Computer Interface (bbci)—towards a new communication channel for online control in gaming applications," *Multimed. Tools Appl.*, vol. 33, no. 1, pp. 73–90, Feb. 2007.
- [35] M. Kleiner, D. Brainard, and D. Pelli, "What's new in Psychtoolbox-3?" *Perception ECV Abstract Suppl.*, vol. 36, p. 14, Jan. 2007.